The British Journal of Radiology, 85 (2012), e899–e905

Simultaneous irradiation of the breast and regional lymph nodes in prone position using helical tomotherapy

K KAINZ, PhD, J WHITE, MD, G-P CHEN, PhD, J HERMAND, CMD, M ENGLAND, MD and X A LI, PhD

Department of Radiation Oncology, Medical College of Wisconsin, Milwaukee, WI, USA

Objective: We investigated dosimetric advantages of using helical tomotherapy to simultaneously irradiate the breast and regional lymph nodes for patients positioned prone, and compared tomotherapy plan qualities for the prone position with those previously published for the supine position.
Methods: Tomotherapy plans for 11 patients (5 left breast, 6 right) simulated with the involved breast suspended downward were generated. Each target (ipsilateral breast and supraclavicular, axillary and internal mammary chain nodes) was to receive 45 Gy.
Results: For targets, $V_{40.5} \geq 99.9\%$ and $V_{42.8} \geq 99.5\%$ for all patients, where $V_{40.5}$ and $V_{42.8}$ denote the relative target volume receiving at least 40.5 and 42.8 Gy, respectively. The targets' maximum dose was, on average, approximately 49.5 Gy. The mean doses to the contralateral lung and heart were lower for right-breast cases (2.8 Gy lung, 2.7 Gy heart) than for left-breast cases (3.8 Gy lung, 8.7 Gy heart). Mean organ doses to the ipsilateral lung (9.3 Gy) and contralateral breast (2.3 Gy) from the prone breast tomotherapy plans were similar to those reported for conventional radiotherapy techniques. For the left breast with regional nodes, tomotherapy plans for prone-positioned patients yielded lower mean doses to the contralateral breast and heart than previously reported data for tomotherapy plans for supine-positioned patients.
Conclusion: Helical tomotherapy with prone breast positioning can simultaneously cover the breast and regional nodes with acceptable uniformity and can provide reduced mean dose to proximal organs at risk compared with tomotherapy with supine position. The similarity of plan quality to existing data for conventional breast radiotherapy indicates that this planning approach is appropriate, and that the risk of secondary tumour formation should not be significantly greater.

Received 31 March 2011
Revised 8 December 2011
Accepted 12 December 2011

DOI: 10.1259/bjr/18685881

For breast cancer patients with large, pendulous breasts, radiation therapy administered with the patient in the prone position can be advantageous [1], in that it may provide favourable dose distributions for the target volumes and organs at risk (OARs) [2–4], reduce the respiration-induced component of anterior patient motion over that for supine positioning [5] and also further separate the lumpectomy site from the lung and heart [6]. However, for advanced stage patients with node-positive disease, using conventional techniques (*e.g.* abutted photon and electron fields) to simultaneously irradiate the ipsilateral breast and regional lymph nodes presents some technical challenges. Among these are limited clearance preventing the use of electron beams, the requirement for set-up and shifts with regard to multiple isocentres (and the opportunities for both systematic and random set-up uncertainties that this can introduce) and the resolution of hot and cold isodose spots at the field junctions [7, 8]. These challenges can be overcome using helical tomotherapy [9], a technique in which intensity-modulated radiation is administered to a patient in motion along the rotation axis of a megavoltage X-ray source. The set-up of a patient with respect to a single ''virtual isocentre'' may avoid the uncertainties inherent in multiple patient shifts during the course of treatment. Also, with helical tomotherapy there is no need to irradiate the nodal groups separately from the ipsilateral breast; this enables more contiguous and uniform dose coverage along the entire extent of the disease, over an arbitrarily long extent in the superior–inferior direction. A further advantage of commercial helical tomotherapy systems is that they are equipped with megavoltage CT (MVCT) capability, which can further reduce set-up uncertainties prior to treatment by registering a pre-treatment MVCT image with the kilovoltage CT (kVCT) image that was used for treatment planning [10, 11]. Given reports of greater set-up uncertainty for prone-positioned patients than for supine patients [12], pre-treatment image guidance to correct for this may be warranted for prone breast treatments. Feasible treatment plans have been reported when applying tomotherapy planning to the whole breast [13–15] and to the whole breast and regional nodes [16] for supine-positioned patients, as well as for partial breast irradiation [17–20].

In this study, we evaluated the capability of helical tomotherapy to irradiate, during the same treatment session with the patient set up to a single isocentre, the ipsilateral breast and the key regional lymph node

Address correspondence to: Dr X Allen Li, Department of Radiation Oncology, Medical College of Wisconsin, 8701 Watertown Plank Road, Milwaukee WI 53226, USA. E-mail: ali@mcw.edu
This work was supported in part by a research grant from the Susan G. Komen Breast Cancer Foundation.

groups with the patient positioned prone, while restricting the dose to nearby OARs to clinically acceptable levels. To evaluate whether the risk of inducing secondary cancers from a tomotherapy treatment to the prone-positioned breast and regional nodes would be similar to that expected using conventional treatments, we compared the mean OAR doses from our plans with a previously published follow-up study of breast cancer patients, some of whom received radiotherapy via conventional techniques (*i.e.* tangents and separate nodal fields). To determine whether positioning breast patients prone instead of supine would yield improved OAR dose sparing for some organs, we compared our plans with those from a previous study investigating helical tomotherapy planning to the breast and regional nodes for supine-positioned patients.

Methods and materials

Patient image data sets used for treatment planning

We generated helical tomotherapy treatment plans based upon the kVCT image data from 11 prone-positioned breast patients who had been previously treated using conventional fixed gantry radiotherapy at our clinic. Note that for these patients only the ipsilateral breast was treated; lymph node coverage was not part of the treatment plan, and thus the patients were not CT imaged with nodal coverage in mind. The kVCT image sets were acquired with the patient lying prone, with the ipsilateral (involved) breast suspended downward and the contralateral breast pushed laterally away from the ipsilateral breast. This configuration was achieved by placing two Styrofoam blocks, each approximately 25-cm thick, between the patient and the table, with one block superior to the breasts and the other block inferior to them. Both blocks were indexed to the treatment couch. A Plexiglas plate, with an aperture to accommodate the ipsilateral breast, was placed atop the Styrofoam boards; the contralateral breast rested atop this Plexiglas plate. The patient's arms were positioned superior to the head; the arms and neck rested within a Vac-Lok™ (MedTec Inc., Orange City, IA) or alpha cradle that was placed between the patient's arms and the superior Styrofoam board. The left breast was suspended for five patients and the right breast for the other six. Among the 11 patients, the average ipsilateral breast volume was $1193 \pm 648\,cm^3$ and ranged from 504 to $2530\,cm^3$.

Regions of interest and planning criteria

Our target structures contoured within our image sets included the ipsilateral whole breast, axillary lymph nodes, supraclavicular lymph nodes and internal mammary chain (IMC) lymph nodes. For the ipsilateral breast contours, the anterior border was 5 mm interior to the skin surface; the posterior border extended to the pectoral muscle; the superior border extended to the axial level of the humeral head; and the inferior border extended to the axial level of the xiphoid process. Wires were not placed upon the skin surface to delineate breast tissue prior to CT simulation. The axillary and supraclavicular nodes were contoured around the nodal structures as apparent on the kVCT images. The IMC nodes were contoured as a 5-mm-diameter contour circumscribing the ipsilateral IMC vessel. Our planning goal was to cover at least 95% of each target structure to 45 Gy in 25 fractions, with $\pm 5\%$ dose uniformity; thus, we sought to keep the maximum point dose below 47.3 Gy, and the minimum point dose above 42.8 Gy. The cumulative dose–volume histogram (DVH) objectives are summarised in the first three columns of Table 1. Neither lumpectomy site contours nor lumpectomy site boosts were incorporated in the treatment planning process.

The following organs were contoured as OAR structures. The contralateral breast's anterior border was drawn 5 mm inward from the skin surface, its posterior border extended to the pectoral muscle, and its superior and inferior extents were the same as those for the ipsilateral breast. The ipsilateral and contralateral lungs were autocontoured individually, without further subdivision. The heart was contoured from the inferior edge of the aortic arch to the base of the heart, with the great vessels excluded. The spinal cord, oesophagus and thyroid were contoured in every kVCT slice where they were apparent.

DVH plan constraints for these OAR structures are summarised in the first three columns of Table 2. These values relate to the DVH constraints that were applied within the tomotherapy treatment planning system, in an effort to achieve OAR doses as low as possible. Although these criteria were not drawn directly from any particular pre-existing protocol study specific to breast and regional nodal radiotherapy, we will show that using these plan criteria led to final mean OAR doses that are consistent with those from the conventional breast-plus-nodes radiotherapy treatments reported in the National Cancer Institute Surveillance, Epidemiology, and End Results (NCI-SEER) Program analyses by Berrington de Gonzalez et al [21]. That study also cited rates of secondary cancers attributable to the use of radiation therapy; thus, secondary cancer rates from our tomotherapy plans are expected to be similar to rates observed from conventional radiotherapy techniques. We will also show that our plan criteria led to final mean OAR doses that are either similar to or slightly improved upon those reported by Goddu et al [16]. That study presented results of tomotherapy plans generated for supine patients, and also covered the ipsilateral breast and regional lymph nodes; this will illustrate potential dosimetric benefits, with regard to some OARs, when using prone positioning instead of supine positioning for tomotherapy breast treatments.

Treatment planning techniques

Helical tomotherapy plans were generated using the TomoTherapy® Hi-Art System (TomoTherapy Inc., Madison, WI). For all plans, the size of the jaw aperture in the longitudinal direction (along the direction of table motion) was 2.5 cm and the pitch was set to 0.43, yielding a beam-intensity resolution of 1.1 cm in the longitudinal direction. The specific choice of pitch was

Table 1. Helical tomotherapy treatment planning constraints for the four target structures

Target structure	Dose–volume parameter	Plan criteria	$\mu \pm \sigma$ all	$\mu \pm \sigma$ left	$\mu \pm \sigma$ right
Ipsilateral breast	V_{45} (%)	≥95.0	89.2 ± 4.0	87.9 ± 5.4	90.4 ± 2.5
	$V_{40.5}$ (%)		100.0 ± 0.1	100.0 ± 0.0	100.0 ± 0.1
	$V_{42.8}$ (%)		99.9 ± 0.2	100.0 ± 0.1	99.9 ± 0.3
	d_{max} (Gy)	<47.3	49.5 ± 1.2	49.1 ± 0.8	49.8 ± 1.4
	d_{min} (Gy)	>42.8	39.4 ± 4.8	40.3 ± 2.0	38.6 ± 6.5
SCV LNs	V_{45} (%)	≥95.0	93.5 ± 5.9	89.8 ± 6.6	96.7 ± 3.0
	$V_{40.5}$ (%)		99.9 ± 0.2	100.0 ± 0.0	99.9 ± 0.3
	$V_{42.8}$ (%)		99.6 ± 0.8	99.9 ± 0.2	99.5 ± 1.1
	d_{max} (Gy)	<47.3	49.0 ± 1.1	48.2 ± 0.5	49.7 ± 1.0
	d_{min} (Gy)	>42.8	42.9 ± 2.7	43.7 ± 1.8	42.1 ± 3.3
Axillary LNs	V_{45} (%)	≥95.0	94.7 ± 5.0	91.7 ± 5.9	97.1 ± 2.6
	$V_{40.5}$ (%)		100.0 ± 0.1	100.0 ± 0.0	99.9 ± 0.2
	$V_{42.8}$ (%)		99.8 ± 0.4	100.0 ± 0.0	99.6 ± 0.6
	d_{max} (Gy)	<47.3	49.0 ± 1.7	47.9 ± 0.6	50.0 ± 1.8
	d_{min} (Gy)	>42.8	42.4 ± 3.0	42.6 ± 2.9	42.4 ± 3.2
IMC LNs	V_{45} (%)	≥95.0	91.2 ± 7.0	85.6 ± 6.3	95.9 ± 3.1
	$V_{40.5}$ (%)		99.9 ± 0.2	100.0 ± 0.0	99.9 ± 0.2
	$V_{42.8}$ (%)		99.5 ± 0.8	99.7 ± 0.4	99.3 ± 1.0
	d_{max} (Gy)	<47.3	48.6 ± 3.8	48.1 ± 0.4	49.0 ± 5.3
	d_{min} (Gy)	>42.8	44.2 ± 3.2	43.4 ± 0.9	44.9 ± 4.4

IMC, internal mammary chain; LN, lymph node; SCV, supraclavicular.

Dose–volume parameters: relative volume of the target structure to receive at least 45, 40.5 and 42.8 Gy (V_{45}, $V_{40.5}$ and $V_{42.8}$, respectively), the maximum point dose (d_{max}) and the minimum point dose (d_{min}).

Also shown are the dose–volume parameters achieved from our treatment planning study; these values are expressed as the average (μ) and standard deviation (σ) over all 11 cases, over the 5 left-breast cases only and over the 6 right-breast cases only.

motivated by Kissick et al [22], and considered appropriate to minimise ''threading'' of the dose distribution due to overlaps at the junctions of the helical-shaped radiation field. Over the first 10–15 iterations, DVH objective values were set for only the target structures; the OAR DVH objectives were kept minimal. This enabled a view of the ''best case scenario'' with regard to target structure dose coverage uniformity. In intervals of every 10–15 iterations thereafter, the DVH objectives were adjusted for one of the OAR structures, and the progress of subsequent DVH modification was monitored. Objective values were adjusted at the high-dose region of the DVH first, working progressively toward lower dose points on the DVH thereafter. No supplementary regions of interest were drawn to bias dose towards or away from a particular region. For some of the plans, it was necessary to reduce the OAR dose by designating the structure as a ''directional block'' (for which only exit dose primary beam trajectories are allowed) or as a ''complete block'' (for which no primary beam trajectory can pass through the OAR). During optimisation, if the setting of DVH point objectives (an upper limit to the maximum point dose, and an upper limit to the OAR volume encompassed by a given dose) did not appear to reduce the OAR dose, that OAR was then designated as a directional block, and optimisation was attempted again. If the OAR's dose still did not adequately decrease, that OAR was then designated as a complete block. Among our 11 cases, we found that complete blocking was required for the contralateral breast for 2 cases and for the heart for 1 (right breast) case. Directional blocking was required for the contralateral breast for two other cases, for the heart for two other (left breast) cases and to the contralateral lung for one case. Not all plans required directional or complete blocking. A final treatment plan emerged after approximately 100–300 iterations in total, depending upon the particular patient case.

Results

For a dose per fraction of 1.8 Gy, the time per fraction to administer a typical helical tomotherapy treatment as calculated by the tomotherapy planning system was on average 11.2 ± 1.7 min, and ranged from 8.2 to 13.3 min. The number of monitor units (MU) per fraction was on average 9649 ± 1507, and ranged from 7053 to 11 489. For our tomotherapy planning and delivery system, 1 MU is equivalent to a dose of 1 cGy at isocentre (85 cm from the TomoTherapy X-ray target) for a field size of 5 × 40 cm at isocentre and a depth of 1.5 cm (the depth of the maximum dose for the TomoTherapy 6 MV beam).

Figure 1 shows a set of cumulative DVHs for a typical helical tomotherapy plan to irradiate the prone breast (the left breast, in this case) and ipsilateral nodal groups. Among the general features of the DVHs for these plans is that the doses to the contralateral lung and contralateral breast can be restricted to levels consistent with scatter dose. For one of the right-breast patients, isodose distributions illustrating the simultaneous 45 Gy coverage of the target structures are shown in Figure 2a for the ipsilateral breast and IMC nodes, and in Figure 2b for the supraclavicular nodes.

The capability of our helical tomotherapy plans to uniformly cover all of the target groups is summarised by Table 1, which presents V_{45}, $V_{40.5}$ (90% of prescribed dose), $V_{42.8}$ (95% of prescribed dose), the maximum point

Table 2. Helical tomotherapy treatment planning constraints for the dose–volume parameters of each of the organ-at-risk (OAR) structures

OAR structure	Dose–volume parameter	Plan constraint in TPS	μ ± σ all	μ ± σ left	μ ± σ right	μ (range)[a]
Ipsilateral lung	V_{20} (%)		12.2 ± 9.9	15.1 ± 11.3	9.7 ± 8.9	
	V_{10} (%)		30.3 ± 8.8	32.7 ± 9.4	28.3 ± 8.6	
	V_5 (%)	<45.0	52.9 ± 13.0	54.4 ± 18.8	51.7 ± 6.9	
	Mean dose (Gy)		9.3 ± 2.6	10.0 ± 3.0	8.8 ± 2.2	10.0 (1.4–42.0)
Contralateral lung	V_{20} (%)		0.0 ± 0.0	0.0 ± 0.0	0.0 ± 0.0	
	V_{10} (%)		0.5 ± 0.9	0.8 ± 1.4	0.2 ± 0.2	
	V_5 (%)	<15.0	16.0 ± 9.8	17.8 ± 10.1	14.6 ± 10.1	
	Mean dose (Gy)		3.3 ± 0.8	3.8 ± 0.6	2.8 ± 0.8	1.1
Cord	d_{max} (Gy)	<20.0	17.3 ± 6.0	16.3 ± 7.3	18.1 ± 5.4	
	V_{10} (%)	<10.0	8.1 ± 7.3	4.4 ± 4.4	11.2 ± 8.2	
Oesophagus	V_5 (%)	<30.0	32.9 ± 13.3	40.9 ± 16.1	26.2 ± 5.3	
	Mean dose (Gy)		7.0 ± 2.1	8.7 ± 0.9	5.6 ± 1.6	5.6 (1.2–19.0)
Thyroid	V_{20} (%)	<40.0	41.8 ± 10.0	46.5 ± 6.4	37.9 ± 11.2	
	Mean dose (Gy)		20.7 ± 2.7	22.6 ± 1.3	19.1 ± 2.6	10.0 (6.0–25.0)
Contralateral breast	V_5 (%)	<5.0	1.3 ± 1.4	1.7 ± 2.0	0.9 ± 0.7	
	Mean dose (Gy)		2.3 ± 0.9	2.4 ± 1.0	2.3 ± 1.0	1.2 (0.8–4.4)
Heart	V_{25} (%)	Left: <9; Right: 0		1.7 ± 2.5	0.0 ± 0.0	
	V_{10} (%)	Left: <30; Right: 0		22.4 ± 7.6	0.1 ± 0.1	
	Mean dose (Gy)			8.7 ± 1.3	2.7 ± 1.1	2.5 (1.0–6.0)

d_{max}, maximum point dose; d_{min}, minimum point dose; TPS, treatment planning system.
For the heart, separate plan criteria were defined for left-breast and right-breast cases. Also shown are the dose–volume parameters achieved from our treatment planning study [relative volume of the target structure to receive at least 45, 40.5 and 42.8 Gy (V_{45}, $V_{40.5}$ and $V_{42.8}$)] these values are expressed as the average (μ) and standard deviation (σ) over all 11 cases, over the 5 left-breast cases only and over the 6 right-breast cases only.
[a]Selected mean organ doses reported by Berrington de Gonzalez et al [21].

dose and the minimum point dose averaged over all 11 patients and over the left-breast and right-breast patients exclusively. V_{45}, $V_{40.5}$, and $V_{42.8}$ denote the relative target volume receiving at least 45, 40.5 and 42.8 Gy. OAR sparing is similarly summarised in Table 2, which presents for our chosen OAR DVH evaluation points

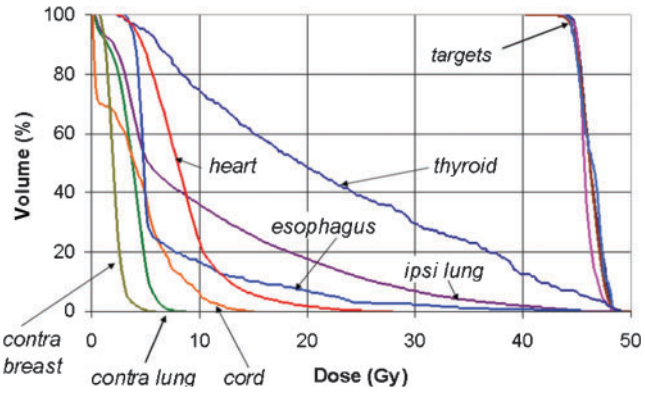

Figure 1. A set of dose–volume histograms for a typical helical tomotherapy plan to irradiate the whole breast and regional lymph nodes, illustrating the uniformity of target coverage and the degree of organ-at-risk sparing. Contra, contralateral; ipsi, ipsilateral.

the average values over all patients and over left-breast and right-breast patients exclusively.

In Table 3, we compare the OAR mean doses from our tomotherapy plans for prone-positioned patients with the results reported by Goddu et al [16]. In the latter study, helical tomotherapy plans (using a planning system identical to our own) were generated for 10 supine-positioned patients, to cover the left-sided breast, axillary nodes, supraclavicular nodes and IMC nodes. As their prescription dose was 50.4 Gy, we applied a scale factor of 45/50.4 to their reported mean organ doses for the ipsilateral and contralateral lungs, contralateral breast and heart. The average planning target volume (PTV) among their 10 cases (5 chest wall, 3 intact breast and 2 breast implant) was 1189 cm^3, which is similar to that from our prone data set.

Discussion

Target coverage

Among the helical tomotherapy plans and for each of the target structures, on average $V_{40.5}$ was ≥99.9% and $V_{42.8}$ was ≥99.5%. V_{45} tended to be somewhat lower than

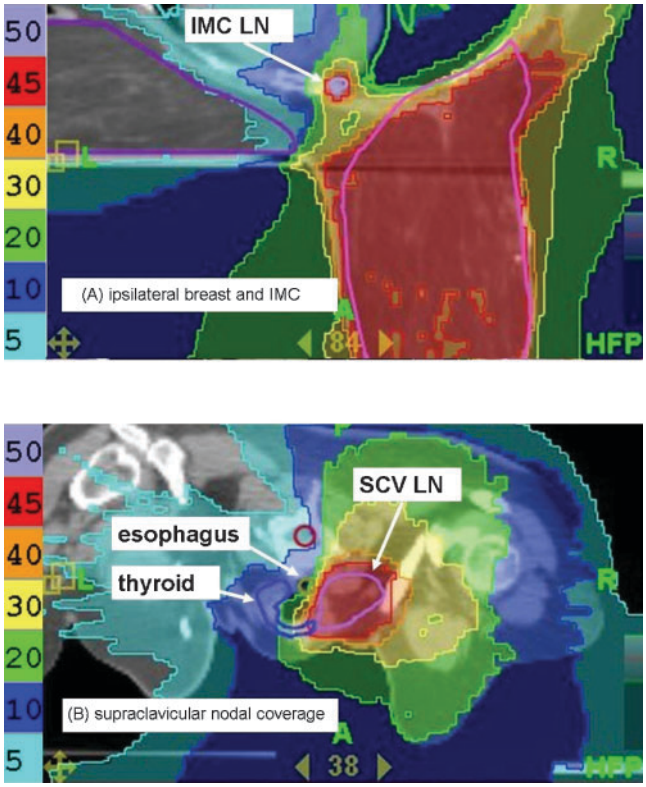

Figure 2. One of the right-breast patient image sets showing the helical tomotherapy plan's isodose coverage of (a) the ipsilateral breast and internal mammary chain (IMC) lymph nodes (LNs) and (b) the supraclavicular (SCV) nodes. The numbers in the above figures denote the isodose values in Gray. Note the sparing of the contralateral breast within the helical tomotherapy plan. The dose avoidance of the cord, oesophagus and thyroid were acceptable.

our objective of 95%, owing to a slight decrease in the calculated dose upon the fractionation calculation within the TomoTherapy planning system software. The minimum point dose to the target structures was, on average, similar to our planning guideline of 42.8 Gy for the nodal targets, but for the ipsilateral breast the minimum point dose was somewhat lower, 39.4 Gy on average; however, the results for $V_{42.8}$ indicate that the volume of the 95% cold spot within any given target volume is only approximately 0.5% of the total volume of the target structure. Our maximum point dose objective (105% of the prescribed dose) was not met for any target structure; on average, the maximum point dose was at most 49.5 Gy, which is 111% of the prescription dose, and among individual plans it ranged from 107% to 114%. This is similar to, although slightly higher than, the maximum point doses to the PTV for supine-breast tomotherapy planning as reported by Goddu et al [16]; in that study, the maximum point dose was on average 109% and ranged from 107% to 112%.

Organ-at-risk sparing

A primary limitation for the use of helical tomotherapy to treat the prone breast is the difficulty in restricting the low-dose coverage to the ipsilateral lung. As indicated in Table 2, although the conventional DVH point quantities for V_{20} [23] and V_{10} [24] for the ipsilateral lung were respected, our average V_5 value was approximately 52.9%, and tends to be independent of left-sided or right-sided cases. Among all patients, the ipsilateral lung V_5 ranged from 36.7% to 86.3%. Although we could achieve $V_5 \leq 60\%$ for nine of our tomotherapy plans, the high V_5 is of concern given observations of V_5 as a predictor for post-treatment respiratory complication [25, 26].

The mean dose to the ipsilateral lung, compiled among all cases and among left-breast and right-breast cases individually, is also given in Table 2; according to Student's *t*-test (assuming two-tailed distributions with unequal variance), no statistically significant difference in mean dose to the ipsilateral lung for left-breast plans *vs* right-breast plans was observed ($p=0.46$). Previous reports of long-term follow-up of breast cancer patients have demonstrated an increased risk of lung cancer for patients receiving breast-conserving radiation therapy via conventional techniques. Clarke et al [27] reported a risk ratio, irradiated *vs* not irradiated, of 1.61 (standard error 0.18). Berrington de Gonzalez et al [21] reported the results from an analysis of breast cancer patients within the US NCI-SEER Program registry; a subset of those patients was treated with tangential fields to the ipsilateral breast along with supraclavicular fields. For that subset, Table A1 of their report [21] summarised the mean organ dose to critical structures, including the oesophagus, ipsilateral lung, contralateral lung, thyroid and contralateral breast; the averages of these mean organ doses among their patients are listed in Table 2. Among our tomotherapy planned cases, the ipsilateral lung mean dose (9.3 ± 2.6 Gy, range 5.5–14.4 Gy) was consistent with both the average and the range of the mean ipsilateral lung dose reported in the SEER analyses (average 10.0 Gy, range 1.4–42.0 Gy). The SEER analyses cite a relative risk of 1.45 [95% confidence interval (CI) 1.35–1.58] for developing secondary cancers in the lung, oesophagus, pleura, bone or soft tissue, approximately 80% of which are lung cancers; they reported 8 excess cases (95% CI 6–9) per 10 000 person-years of solid tumours in this category. We should expect that the probability of secondary lung cancers resulting from helical tomotherapy treatments to the prone breast and regional nodes would be similar to the rates estimated from the SEER data.

A potential limitation of the tomotherapy technique is the difficulty in controlling the low-dose coverage of the oesophagus. Table 2 shows that the V_5 value, averaged over all patients, was 32.9%, which exceeds our criterion of 30%. A possible explanation for this is the proximity of the oesophagus to the supraclavicular nodes, as illustrated in Figure 2b. Among left-breast patients, the oesophagus V_5 was $40.9 \pm 16.1\%$ on average, and among right-breast patients it was $26.2 \pm 5.3\%$; however, this difference was not statistically significant ($p=0.11$). Controlling dose to the thyroid is also a challenge, given its proximity to the supraclavicular nodes; among our plans, the thyroid V_{20} was on average $41.8 \pm 10.0\%$. The mean thyroid dose among left-breast cases was 22.6 ± 1.3 Gy, and among right-breast cases was 19.1 ± 2.6 Gy. This difference was slightly statistically significant ($p=0.01$). Among all of our plans, the maximum point dose to the cord was on average

Table 3. Mean organ doses from our helical tomotherapy plans for prone-positioned patients compared with the results reported by Goddu et al [16] for helical tomotherapy plans to treat the left breast and regional lymph nodes to 50.4 Gy for supine-positioned patients

		Mean organ dose (Gy), prone plans (current study)		Mean organ dose (Gy), supine plans ([16]) scaled to 45 Gy radiation dose	
OAR structure	Treated side	$\mu \pm \sigma$	Range	$\mu \pm \sigma$	Range
Ipsilateral lung	Left	10.0 ± 3.0	6.6–14.4	10.6 ± 1.3	8.6–13.2
	Right	8.8 ± 2.2	5.5–11.7		
Contralateral lung	Left	3.8 ± 0.6	2.8–4.3	3.8 ± 0.9	1.9–5.1
	Right	2.8 ± 0.8	1.6–3.9		
Contralateral breast	Left	2.4 ± 1.0	1.0–3.4	3.8 ± 0.6	2.8–4.6
	Right	2.3 ± 1.0	0.6–3.3		
Heart	Left	8.7 ± 1.3	6.8–10.1	10.9 ± 1.6	8.8–13.8
	Right	2.7 ± 1.0	0.6–3.3		

μ, average; σ, standard deviation; OAR, organ at risk.
The tabulated values were scaled down by a factor of (45 Gy)/(50.4 Gy).

17.3 ± 6.0 Gy, and ranged from 10.4 to 28.9 Gy for individual plans.

For the heart, the V_{25} DVH objective was satisfied for both left-breast and right-breast cases. However, while our V_{10} planning objective was satisfied for left-breast cases, for right-breast cases the average V_{10} for the heart was 0.1%. Among left-breast cases the mean heart dose was 8.7 ± 1.3 Gy, while for right-breast cases it was 2.7 ± 1.1 Gy; Student's *t*-test indicated high statistical significance ($p=0.00004$). Although isodose lines of the order of 5 Gy can be kept out of the heart, our original goal of total avoidance for the heart was not met for right-sided cases.

For the contralateral lung, among the cardinal dose–volume parameters considered, only V_5 was significant, about 16% on average; contralateral lung V_5 was lower for right-breast cases than for left-breast cases. We found that among our left-breast cases the mean dose to the right lung (3.8 ± 0.6 Gy) was slightly higher than the mean dose to the left lung (2.8 ± 0.8 Gy) for right-breast cases. Student's *t*-test analysis yielded $p=0.05$, which indicates slight statistical significance. We attributed the mean dose difference to more stringent dose avoidance to the heart when generating right-breast plans; for those cases, the contralateral lung is proximal to the heart.

Our DVH-based plan criterion for the contralateral breast was easily met by our helical tomotherapy plans. The V_5 dose to the contralateral breast was 1.3%, on average, over all patients. Among all plans, the mean dose to the contralateral breast was on average 2.3 ± 0.9 Gy, and ranged from 0.6 to 3.4 Gy. No statistically significant difference was seen in the mean contralateral breast dose for left-sided *vs* right-sided cases ($p=0.86$). The mean organ doses from our tomotherapy plans are consistent with the range of doses reported from the SEER analyses [21], although for most OARs the tomotherapy mean organ dose is on average slightly higher. The SEER analyses calculated the likelihood of radiation-induced excess secondary cancers by comparisons with patients in its database who were not treated with radiation. SEER reported 5 excess contralateral breast cancer cases (95% CI 2–7) per 10 000 person-years arising from radiotherapy. The mean contralateral breast dose from our plans (2.3 ± 0.9 Gy) is consistent with the range of doses reported in the SEER analyses (0.8–4.4 Gy). The similarity of our OAR mean organ doses to the SEER cases suggests that (1) our tomotherapy planning criteria are appropriate and (2) the risk of inducing secondary cancers from a helical tomotherapy technique would be similar to the rate of excess cases reported from SEER.

The mean organ doses for our prone-positioned tomotherapy plans for our five left-sided treatments compare favourably with those for the supine-positioned plans reported by Goddu et al [16]. Averaged among all patients, the mean organ doses to the ipsilateral lung, contralateral breast and heart are slightly lower for the prone plans than for the supine plans. These results suggest that, if helical tomotherapy is considered to simultaneously treat the left breast and regional nodes, simulation of the patient in the prone position may be dosimetrically advantageous. For the ipsilateral lung, a higher dose might arise from a supine plan owing to curvature of the ipsilateral breast around the chest wall, and that curvature may become more significant for larger breast patients. For the contralateral breast and heart, lower doses might arise from a prone plan owing to increased separation of the ipsilateral breast from these two OARs.

To summarise, for breast cancer patients with advanced stage disease who are simulated in the prone position, helical tomotherapy can simultaneously cover the entire ipsilateral breast and the regional lymph nodes with an acceptable degree of dose uniformity. The similarity of our OAR mean organ doses to those reported in the extensive follow-up study of the SEER Registry suggest that our plan criteria and plan optimisation parameters are appropriate, and that helical tomotherapy treatment to the prone breast and regional lymph nodes is not expected to yield significantly greater risk of secondary tumour formation relative to conventional radiotherapy techniques.

References

1. Mahe M-A, Classe J-M, Dravet F, Cussac A, Cuilliere J-C. Preliminary results for prone-position breast irradiation. Int J Radiat Oncol Biol Phys 2002;52:156–60.
2. Merchant TE, McCormick B. Prone position breast irradiation. Int J Radiat Oncol Biol Phys 1994;30:197–203.
3. Grann A, McCormick B, Chabner ES, Gollamudi SV, Schupak KD, Mychalczak BR, et al. Prone breast

radiotherapy in early-stage breast cancer: a preliminary analysis. Int J Radiat Oncol Biol Phys 2000;47:319–25.
4. Kirby AM, Evans PM, Donovan EM, Convery HM, Haviland JS, Yarnold JR. Prone versus supine positioning for whole and partial-breast radiotherapy: a comparison of non-target tissue dosimetry. Radiother Oncol 2010;96: 178–84.
5. Stepaniak C, Li X, White J, Wilson J. Thoracic organ motion as assessed by 4D CT: prone versus supine. Med Phys 2005;32:1949.
6. Becker SJ, Patel RR, Mackie TR. Accelerated partial breast irradiation with helical tomotherapy: prone or supine setup? Int J Radiat Oncol Biol Phys 2006;66:S230.
7. Podgorsak EB, Gosselin M, Kim TH, Freeman CR. A simple isocentric technique for irradiation of the breast, chest wall and peripheral lymphatics. Br J Radiol 1984;57:57–63.
8. Idzes MHM, Holmberg O, Mijnheer BJ, Huizenga H. Effect of set-up uncertainties on the dose distribution in the match region of supraclavicular and tangential breast fields. Radiother Oncol 1998;46:91–8.
9. Mackie TR, Holmes T, Swerdloff S, Reckwardt P, Deasy JO, Yang J, et al. Tomotherapy: a new concept for the delivery of dynamic conformal radiotherapy. Med Phys 1993;20: 1709–19.
10. Forrest LJ, Mackie TR, Ruchala K, Turek M, Kapatoes J, Jaradat H, et al. The utility of megavoltage computed tomography images from a helical tomotherapy system for setup verification purposes. Int J Radiat Oncol Biol Phys 2004;60:1639–44.
11. Mahan SL, Ramsey CR, Scaperoth DD, Chase DJ, Byrne TE. Evaluation of image-guided helical tomotherapy for the retreatment of spinal metastases. Int J Radiat Oncol Biol Phys 2005;63:1576–83.
12. Kirby AM, Evans PM, Helyer SJ, Donovan EM, Convery HM, Yarnold JR. A randomized trial of supine versus prone breast radiotherapy (SuPr study): comparing set-up errors and respiratory motion. Radiother Oncol 2011;100:221–6.
13. Gonzalez VJ, Buchholz DJ, Langen KM, Olivera GH, Chauhan B, Meeks SL, et al. Evaluation of two tomotherapy-based techniques for the delivery of whole-breast intensity-modulated radiation therapy. Int J Radiat Oncol Biol Phys 2006;65:284–90.
14. Coon AB, Dickler A, Kirk MC, Liao Y, Shah AP, Strauss JB, et al. Tomotherapy and multifield intensity-modulated radiotherapy planning reduce cardiac doses in left-sided breast cancer patients with unfavorable cardiac anatomy. Int J Radiat Oncol Biol Phys 2010;78:104–10.
15. Donovan EM, Ciurlionis L, Fairfoul J, James H, Mayles H, Manktelow S, et al. Planning with intensity-modulated radiotherapy and tomotherapy to modulate dose across breast to reflect recurrence risk (IMPORT HIGH Trial). Int J Radiat Oncol Biol Phys 2011;79:1064–72.
16. Goddu SM, Chaudhari S, Mamalui-Hunter M, Pechenaya OL, Pratt D, Mutic S, et al. Helical tomotherapy planning for left-sided breast cancer patients with positive lymph nodes: comparison to conventional multiport breast technique. Int J Radiat Oncol Biol Phys 2009;73:1243–51.
17. Hui SK, Das RK, Kapatoes J, Olivera G, Becker S, Odau H, et al. Helical tomotherapy as a means of delivering accelerated partial breast irradiation. Technol Cancer Res Treat 2004;3:639–46.
18. Patel RR, Becker SJ, Das RK, Mackie TR. A dosimetric comparison of accelerated partial breast irradiation techniques: multicatheter interstitial brachytherapy, three-dimensional conformal radiotherapy, and supine versus prone helical tomotherapy. Int J Radiat Oncol Biol Phys 2007;68: 935–42.
19. Kainz K, White J, Herman J, Li X. Investigation of helical tomotherapy for partial-breast irradiation of prone-positioned patients. Int J Radiat Oncol Biol Phys 2009;74:275–82.
20. Kainz K, White J, Li X. MVCT-guided partial-breast irradiation in prone position: daily setup uncertainty and dose verification. Med Phys 2008;35:2901.
21. Berrington de Gonzalez A, Curtis RE, Gilbert E, Berg CD, Smith SA, Stovall M, et al. Second solid cancers alter radiotherapy for breast cancer in SEER cancer registries. Br J Cancer 2010;102:220–6.
22. Kissick MW, Fenwick J, James JA, Jeraj R, Kapatoes JM, Keller H, et al. The helical tomotherapy thread effect. Med Phys 2005;32:1414–23.
23. Graham MV, Purdy JA, Emami B, Harms W, Bosch W, Lockett MA, et al. Clinical dose-volume histogram analysis for pneumonitis after 3D treatment for non-small cell lung cancer (NSCLC). Int J Radiat Oncol Biol Phys 1999;45:323–9.
24. Lee HK, Vaporciyan AA, Cox JD, Tucker SL, Putnam JB, Ajani JA, et al. Postoperative pulmonary complications after preoperative chemoradiation for esophageal carcinoma: correlation with pulmonary dose-volume histogram parameters. Int J Radiat Oncol Biol Phys 2003;57:1317–22.
25. Wang SL, Liao Z, Vaporciyan AA, Tucker SL, Liu H, Wei X, et al. Investigation of clinical and dosimetric factors associated with postoperative pulmonary complications in esophageal cancer patients treated with concurrent chemoradiotherapy followed by surgery. Int J Radiat Oncol Biol Phys 2006;64:692–9.
26. Wang S, Liao Z, Wei X, Liu HH, Tucker SL, Hu C-S, et al. Analysis of clinical and dosimetric factors associated with treatment-related pneumonitis (TRP) in patients with non-small-cell lung cancer (NSCLC) treated with concurrent chemotherapy and three-dimensional conformal radiotherapy (3D-CRT). Int J Radiat Oncol Biol Phys 2006;66: 1399–407.
27. Clarke M, Collins R, Darby S, Davies C, Elphinstone P, Evans V, et al. Effects of radiotherapy and of differences in the extent of surgery for early breast cancer on local recurrence and 15-year survival: an overview of the randomized trials. Lancet 2005;366:2087–106.